Supplementary Information for

Synthesis and performances of $ZnCo_2O_4$@$MnMoO_4$ composite for hybrid supercapacitor

Xuan Liao,†[a] Hang Yang,†[a] Xiaolong Hou,[a] Caini Yi,[a] Ying Yang,[a] Guimao Wang,[a] Shuo Wang,[a] Yuping Liu,[a] Changguo Chen,[a] Danmei Yu*[a] and Xiaoyuan Zhou*[b]

[a] School of Chemistry and Chemical Engineering, Chongqing University, Chongqing, 401331, P.R. China

[b] College of Physics, Chongqing University, Chongqing, 401331, P.R. China

† **Co-first author:** Xuan Liao, Hang Yang

Corresponding Authors

***Danmei Yu's** e-mail: yudanmei-1@163.com.

***Xiaoyuan Zhou's** e-mail: xiaoyuan2013@cqu.edu.cn**.**

Notes

The authors declare no competing financial interest

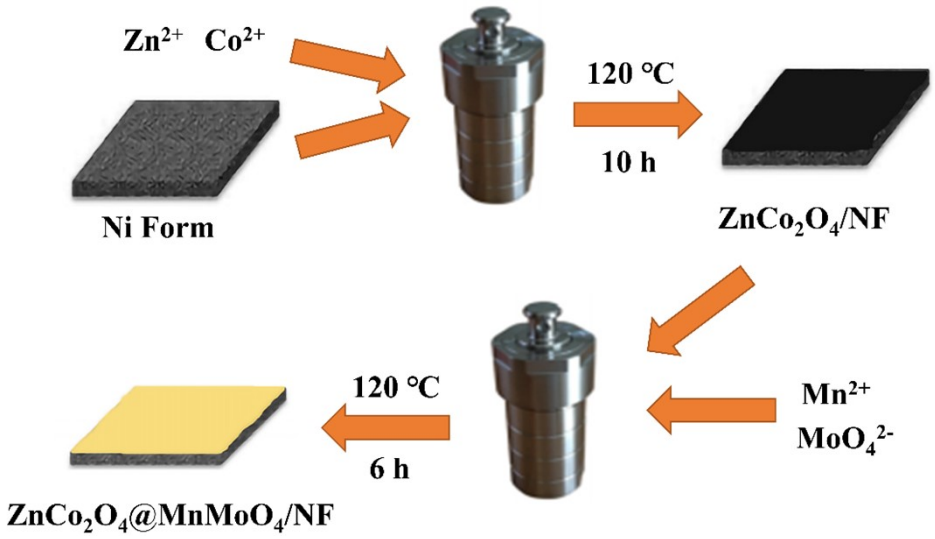

Fig. S1 Schematic illustration of synthesizing hierarchical $ZnCo_2O_4$@$MnMoO_4$/NF electrode.

The optimization of second step hydrothermal time

The second step hydrothermal reaction time has a great influence on the electrochemical properties of the composites. In order to determine the optimal hydrothermal reaction time, the second step hydrothermal reaction time was set as 4, 6, and 9 h when prepared $ZnCo_2O_4$@$MnMoO_4$ composites and named $ZnCo_2O_4$@$MnMoO_4$-1, $ZnCo_2O_4$@$MnMoO_4$-2, and $ZnCo_2O_4$@$MnMoO_4$-3, respectively. The electrochemical performances of prepared composite materials were investigated in a three-electrode system using 3 M KOH as electrolyte, Pt sheet as counter electrode and Hg/HgO as reference electrode.

In order to evaluate the specific capacity of the prepared materials, the GCD tests of $ZnCo_2O_4$@$MnMoO_4$-1, $ZnCo_2O_4$@$MnMoO_4$-2, and $ZnCo_2O_4$@$MnMoO_4$-3 electrodes were performed at a current density of 1 A/g. As shown in Fig. S3(a), the GCD curves of all prepared materials have obvious charging and discharging platforms and are very symmetric, which indicating better electrochemical reversibility. Notably, $ZnCo_2O_4$@$MnMoO_4$-2 has the longest discharge time under

the same condition.

From Eq. (1), the specific capacitances of prepared composites can be calculated. At 2 A/g current density, the specific capacitance of the $ZnCo_2O_4$@$MnMoO_4$-2 is 1628 F/g, while that of $ZnCo_2O_4$@$MnMoO_4$-1 and $ZnCo_2O_4$@$MnMoO_4$-3 are only 960 F/g and 828 F/g. That is, the specific capacitance of $ZnCo_2O_4$@$MnMoO_4$ electrodes is significantly higher than that of $ZnCo_2O_4$@$MnMoO_4$-1 at the same current density. Fig.S3(b) depicts the specific capacitances of $ZnCo_2O_4$@$MnMoO_4$-1, $ZnCo_2O_4$@$MnMoO_4$-2, and $ZnCo_2O_4$@$MnMoO_4$-3 at different current densities. Thus, it can be inferred that $ZnCo_2O_4$@$MnMoO_4$-2 possesses the best electrochemical performance among all prepared composites.

In order to investigate the impedance of the prepared composites, EIS tests of $ZnCo_2O_4$@$MnMoO_4$-1, $ZnCo_2O_4$@$MnMoO_4$-2, and $ZnCo_2O_4$@$MnMoO_4$-3 electrodes were carried out. Fig.S3(c) shows the Nyquist plots of the prepared composite electrodes in the frequency range of 0.01-100 kHz at open-circuit potential. The Nyquist plots mainly consist of semicircles in the high-frequency region and straight lines in the low-frequency region. Normally, the semicircle diameter correlates with the charge-transfer impedance, while the straight-line slope is related to the diffusion impedance of ions. It is noteworthy that the semicircle diameters of all prepared electrodes are very small. But the straight line slope of $ZnCo_2O_4$@$MnMoO_4$-2 is the largest, indicating the smallest diffusion impedance. So $ZnCo_2O_4$@$MnMoO_4$-2 possesses the best ions diffusion and good electrical

conductivity.

In order to study the cycling performance of the prepared composites, $ZnCo_2O_4$@$MnMoO_4$-1, $ZnCo_2O_4$@$MnMoO_4$-2, and $ZnCo_2O_4$@$MnMoO_4$-3 electrodes were charged and discharged for 10,000 cycles at a current density of 10 A/g. According to Fig.S3(d), the capacity retention of $ZnCo_2O_4$@$MnMoO_4$-2 after 10,000 cycles still keeps 69%, while that of $ZnCo_2O_4$@$MnMoO_4$-1 and $ZnCo_2O_4$@$MnMoO_4$-3 is 62% and 57%, respectively. As a result, $ZnCo_2O_4$@$MnMoO_4$-2 possesses the best cycling stability among all prepared composites.

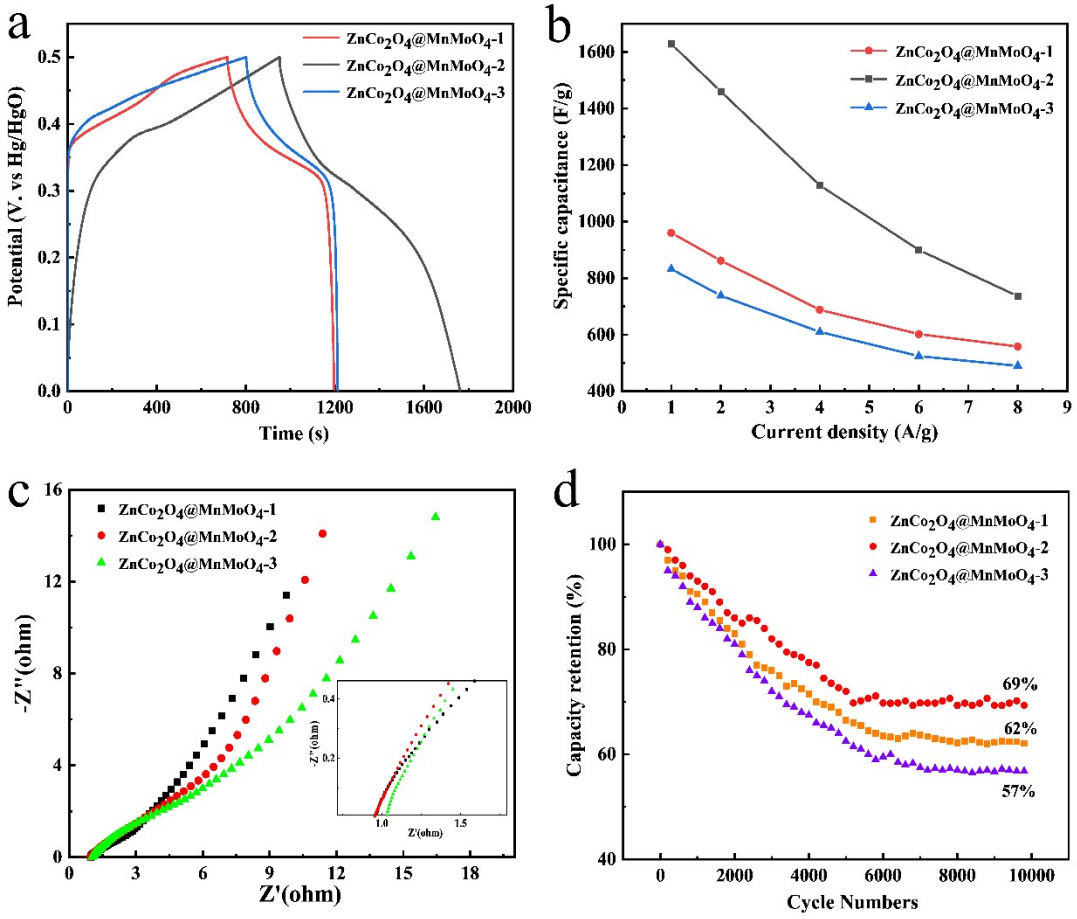

Fig. S2 (a) GCD curves of the prepared composite materials at 1 A/g, (b) The specific capacity change curves of the prepared composite materials with different current densities, (c) Nyquist plots of the prepared composite materials and (d) Cycle performances of the prepared composite materials.

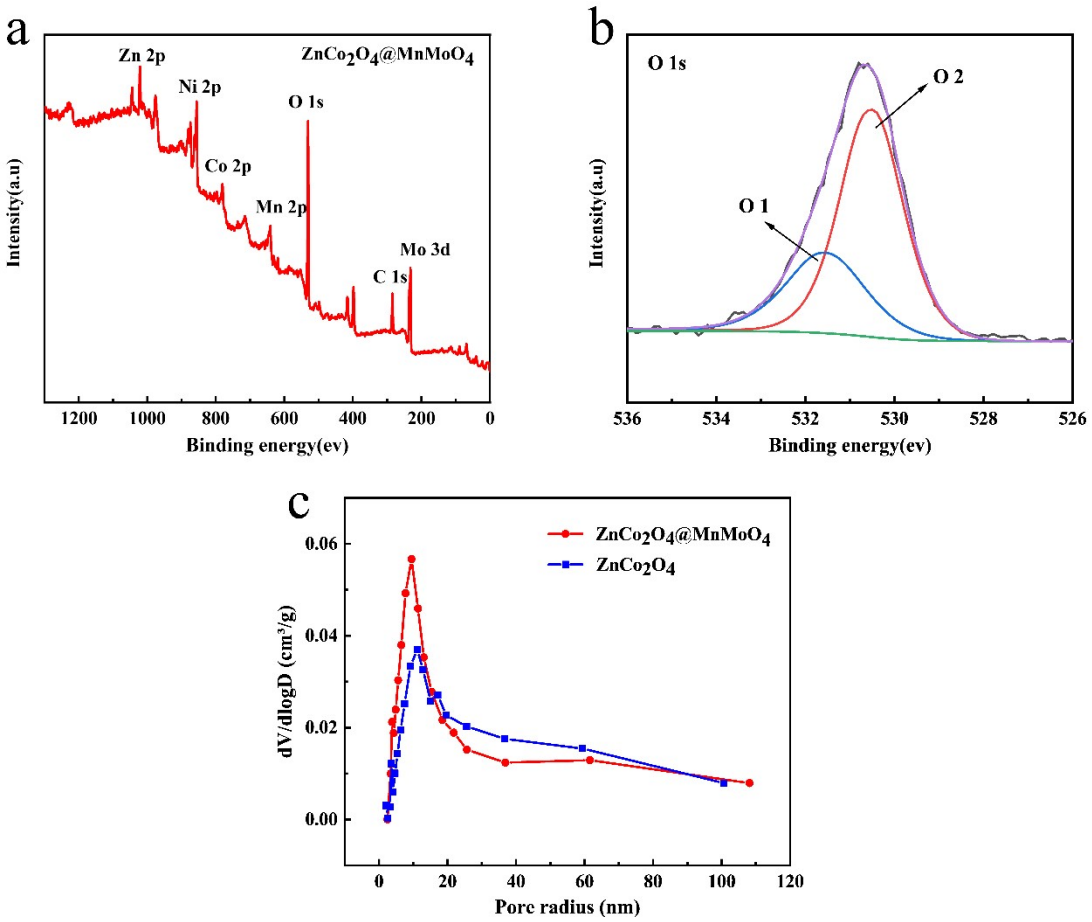

Fig. S3 (a)XPS survey spectra of $ZnCo_2O_4$@$MnMoO_4$ composite, (b) XPS spectra of O 1s and (c) Pore size distribution curves of prepared materials.

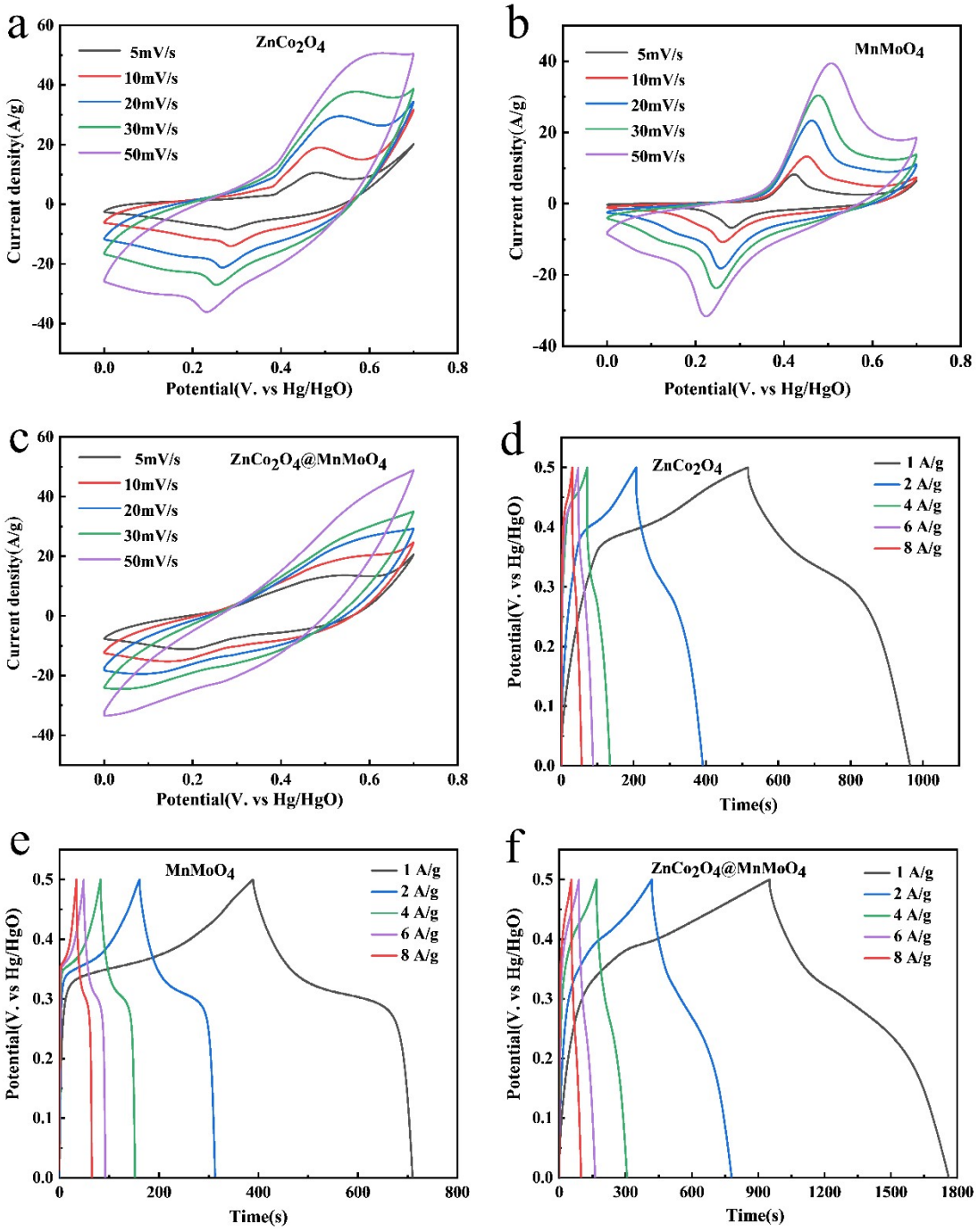

Fig. S4(a-c) CV curves of $ZnCo_2O_4$, $MnMoO_4$ and $ZnCo_2O_4$@$MnMoO_4$ at different san rates, (d-f) GCD curves of $ZnCo_2O_4$, $MnMoO_4$ and $ZnCo_2O_4$@$MnMoO_4$ at different current densities.

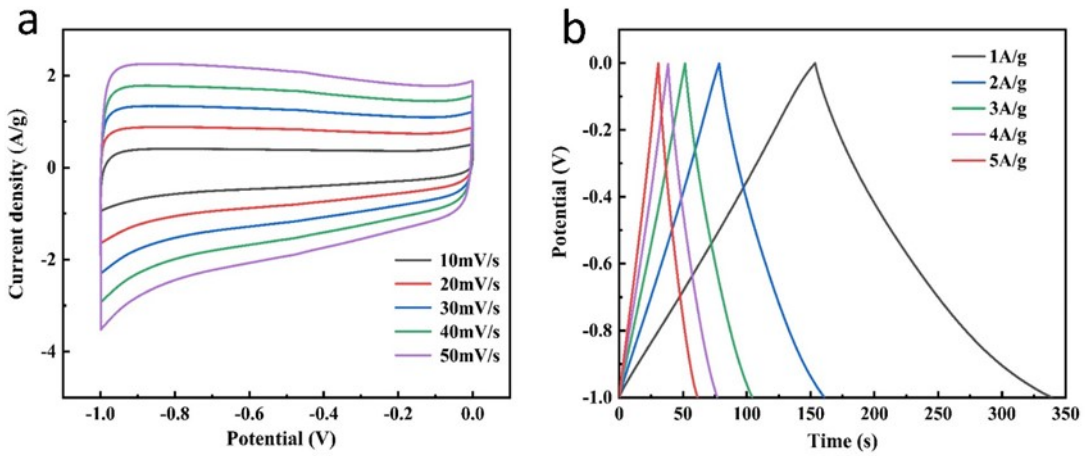

Fig. S5 Electrochemical performances of activated carbon (AC) negative electrode: (a) CV curves, (b) GCD curves.

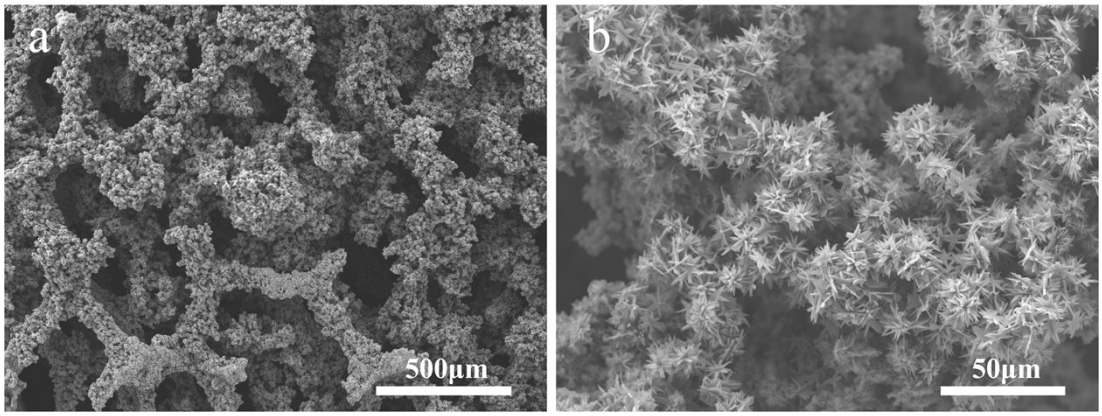

Fig. S6 SEM images of $ZnCo_2O_4$@$MnMoO_4$ electrode material after cycling.

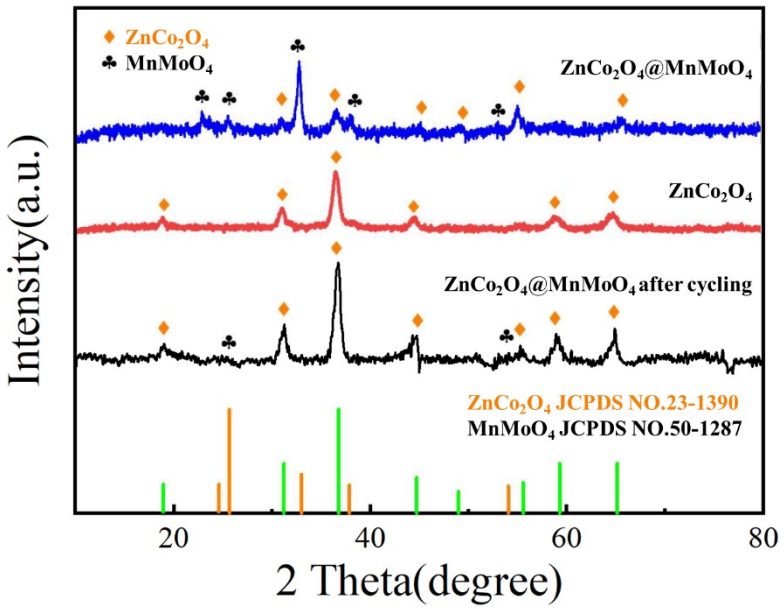

Fig. S7 XRD Patterns of $ZnCo_2O_4$, $ZnCo_2O_4$@$MnMoO_4$ before and after cycling

Table S1. Comparative capacitance of $ZnCo_2O_4$@$MnMoO_4$ with other electrode materials

Electrode	Capacity @1 A/g (F/g)	Reference
MGNs/$ZnCo_2O_4$	960	[37]
$ZnCo_2O_4$/QCs	804	[38]
$ZnCo_2O_4$@$NiCo_2O_4$	1476	[39]
$ZnCo_2O_4$-ZnO	810	[40]
$ZnCo_2O_4$@$MnCo_2O_4$	254	[41]
$ZnCo_2S_4$/$ZnCo_2O_4$	1058	[42]
$ZnCo_2O_4$/CC	150	[43]
ZnO/$ZnCo_2O_4$/NiO	1136	[44]
$ZnCo_2O_4$	900	This work
$MnMoO_4$	644	This work
$ZnCo_2O_4$@$MnMoO_4$	**1628**	**This work**